Functional analysis of parvin and different modes of IPP-complex assembly at integrin sites during *Drosophila* development

Katerina M. Vakaloglou*, Maria Chountala* and Christos G. Zervas‡

Biomedical Research Foundation, Academy of Athens (BRFAA), Division of Genetics, Soranou Efessiou 4, 11527 Athens, Greece

*These authors contributed equally to this work

‡Author for correspondence (czervas@bioacademy.gr)

Accepted 5 March 2012
Journal of Cell Science 125, 3221–3232

doi: 10.1242/jcs.102384

Summary

Integrin-linked kinase (ILK), PINCH and parvin constitute the tripartite IPP complex that maintains the integrin–actin link at embryonic muscle attachment sites (MASs) in *Drosophila*. Here we showed that parvin null mutants in *Drosophila* exhibit defects in muscle adhesion, similar to ILK and PINCH mutants. Furthermore, the identical muscle phenotype of the triple mutant, which for the first time in any organism removed the entire IPP-complex function, genetically demonstrated that parvin, ILK and PINCH function synergistically. This is consistent with the tight localization of the tripartite complex at sites of integrin adhesion, namely MASs in the developing embryo and focal-contact-like structures in the wing epithelium. Parvin contains tandem unconventional calponin-homology (CH) domains separated by a linker sequence, and a less-well conserved N-terminal region. In vivo structure–function analysis revealed that all the domains are essential for parvin function, whereas recruitment at integrin adhesion sites is mediated by two localization signals: one located within the CH2 domain as previously reported, and a second novel signal within the CH1 domain. Interestingly, this site is masked by the linker region between the two CH domains, suggesting a regulatory mechanism to control parvin localization. Finally, whereas in muscles only ILK controls the stability and localization of both PINCH and parvin, in the wing epithelium the three proteins mutually depend on each other. Thus molecular differences exist in the assembly properties of IPP complex in specific tissues during development, where differential modulation of the integrin connection to the cytoskeleton is required.

Key words: ILK, PINCH, Muscle attachment sites, Adhesion, Actin

Introduction

During animal development cells assemble into tissues and establish specific adhesion sites with the surrounding extracellular matrix (ECM). ECM enables the stable attachment of cells and their separation in distinct layers permitting tissue morphogenesis. The integrin family of transmembrane proteins mediate physical contact of cells with the ECM. This connection requires direct binding of the extracellular domain of both the α- and the β-subunit of integrin to their ECM ligands, whereas their small cytoplasmic tails bind a network of proteins to form the integrin adhesome and mediate the link to the actin cytoskeleton (Geiger and Yamada, 2011). The molecular composition of the integrin adhesome network is diverse, highly dynamic and largely determined by the cell type and the physical strength required by the local developmental microenvironment (Wolfenson et al., 2009; Zaidel-Bar et al., 2007).

The tripartite IPP complex containing integrin-linked kinase (ILK), PINCH and parvin is central to the integrin adhesome network (Wickström et al., 2010; Wu and Dedhar, 2001). In invertebrates, the IPP-complex components are encoded by single genes, in contrast to the two PINCH genes and three parvin genes (α-, β- and γ-parvin) in mammals (Legate et al., 2006). The early evolutionary appearance of ancestral IPP-complex components suggest that the IPPb complex may have been one of the first molecular machines used by integrins (Sebé-Pedrós et al., 2010).

ILK plays a central role in the formation of the IPP complex. It contains five tandem ankyrin repeats (ANKRs) followed by a kinase-like domain, and interacts with the β1 and β3 integrin cytoplasmic tails (Hannigan et al., 1996). The ANKRs of ILK bind to PINCH, an adaptor protein containing five LIM domains, whereas the kinase-like domain of ILK binds to parvin, which in turn binds to actin (Legate et al., 2006). Thus, a simple model of IPP-complex function envisages either direct or indirect anchoring of ILK to integrins, with parvin mediating the link to actin. This model is supported by studies showing linear assembly of IPP complex in invertebrates. In *Caenorhabditis elegans*, ILK is required for both parvin and PINCH subcellular localization but not the reverse, and in *Drosophila* ILK is similarly required for PINCH stability and recruitment, although parvin has not been tested (Lin et al., 2003; Norman et al., 2007; Zervas et al., 2011).

In mammalian cells, genetic elimination of one component of the IPP complex results in a significant decrease of the other two members, although some compensation has been observed for parvins and PINCH (Wickström et al., 2011). Moreover, distinct IPP complexes are formed within cells containing different parvin and PINCH members, resulting in different functional properties (Wu, 2004). However, it is unknown whether removing all IPP components enhances the defects of single deletions, and thus whether all components function together or have other individual functions.

Journal of Cell Science

The parvin family was initially identified by sequence similarity to α-actinin. Recent detailed analysis of parvin CH2-domain interactions with the ILK kinase domain and the leucine aspartate (LD)-rich repeats of paxillin suggested that parvin contributes to the assembly of focal adhesions in mammalian cells (Fukuda et al., 2009; Lorenz et al., 2008; Nikolopoulos and Turner, 2000; Olski et al., 2001; Wang et al., 2008). Genetic ablation of α-parvin in mice uncovered its function in vascular morphogenesis as a negative regulator of RhoA/ROCK signaling (Lange et al., 2009; Montanez et al., 2009). However, due to functional compensation by β-parvin, earlier developmental functions of the parvin family were hard to study, possibly explaining why deletion of α-parvin does not phenocopy defects in early embryo development observed with genetic elimination of ILK or PINCH-1 (Li et al., 2005; Sakai et al., 2003). Expression of, γ-parvin is restricted to the hematopoietic system, where it is not essential (Chu et al., 2006).

We previously found that ILK is required to link the actin cytoskeleton to the integrin-containing junctions at embryonic muscle attachment sites (MASs) in *Drosophila*, and PINCH was subsequently shown to be required for the same process (Clark et al., 2003; Zervas et al., 2001). Up to date there have been no genetic studies of the single *Drosophila* parvin gene, resulting in a currently incomplete characterization of IPP-complex function in flies. Here we performed a detailed functional characterization of parvin and the IPP complex in *Drosophila* development by generating a series of specific mutants and analyzing their effects on protein function and localization, in both the MASs of developing embryos and the wing epithelium.

Results

Molecular characterization of *Drosophila* parvin

The Berkeley Drosophila Genome Project identified CG32528 as the single fly parvin, located on the X chromosome at cytogenetic region 18E5–18F1. *Drosophila* parvin protein is 59%, 57% and 42% identical to human β-, α- and γ-parvin, respectively and its domain organization is similar to its mammalian homologs, a novel N-terminal region followed by two unconventional CH domains separated by a linker with unknown function (Fig. 1A).

We engineered two genomic parvin–GFP fusion constructs containing different lengths of the upstream region to monitor the dynamic expression of parvin in the living organism (Fig. 1B). In transgenic flies the ~7.2 kb construct was expressed sufficiently (Fig. 1C, Fig. 2; supplementary material Fig. S1), whereas the ~3.5 kb construct was poorly expressed in embryos (supplementary material Fig. S1). Similar N-terminal tagging of the mammalian parvin does not affect its expression and stability (Olski et al., 2001), suggesting that the longer upstream region of the ~7.2 kb construct likely contains crucial regulatory elements controlling either the level or the spatiotemporal expression of parvin.

Expression of parvin during embryogenesis

To examine the tissue distribution and subcellular localization of endogenous parvin in *Drosophila* development, we raised polyclonal antibodies against the N-terminal region (aa:1–241). On western blots, the antiserum detected a band of the predicted molecular weight (42 kDa) in extracts from wild-type, but not mutant embryos (Fig. 1C). In transgenic embryos expressing parvin–GFP, an additional 70 kDa band corresponding to parvin–GFP was detected (Fig. 1C). We further confirmed the specificity of the antiserum by immunostaining in embryos ectopically expressing the UAS::parvin-GFP transgene under the control of *engrailedGal4* (supplementary material Fig. S2).

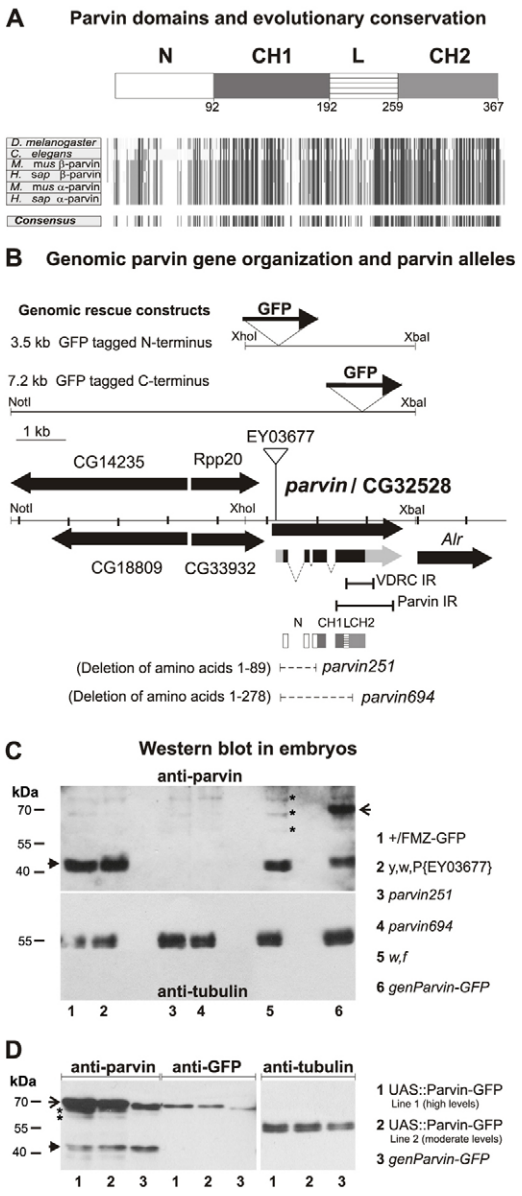

Fig. 1. Molecular organization of *Drosophila* parvin and characterization of parvin mutants. (**A**) Schematic presentation of *Drosophila* parvin domain organization and alignment of parvin protein sequences. Below: lines represent amino acids, shaded to illustrate conservation: black, identical in all species; gray, similar; white, different. (**B**) Engineered genomic parvin–GFP fusion rescue constructs. Genomic parvin gene organization with exons (black boxes), introns (white boxes), transcripts of flanking genes (filled black arrows) and the insertion site of the *EY03677* P-element. The deletions generated in *parvin*^{694} and *parvin*^{251} during imprecise excision are also shown. (**C**,**D**) Parvin protein levels in wild-type, parvin mutants and transgenic flies expressing full-length parvin–GFP driven by mef2Gal4. Western blots of embryo extracts probed with anti-parvin, anti-tubulin (loading control) and anti-GFP. Asterisks (*) indicate non-specific bands; closed arrowhead, the endogenous parvin; open arrow, parvin–GFP.

Parvin–GFP expression from the ~7.2 kb genomic rescue fragment was compared to endogenous parvin detected with

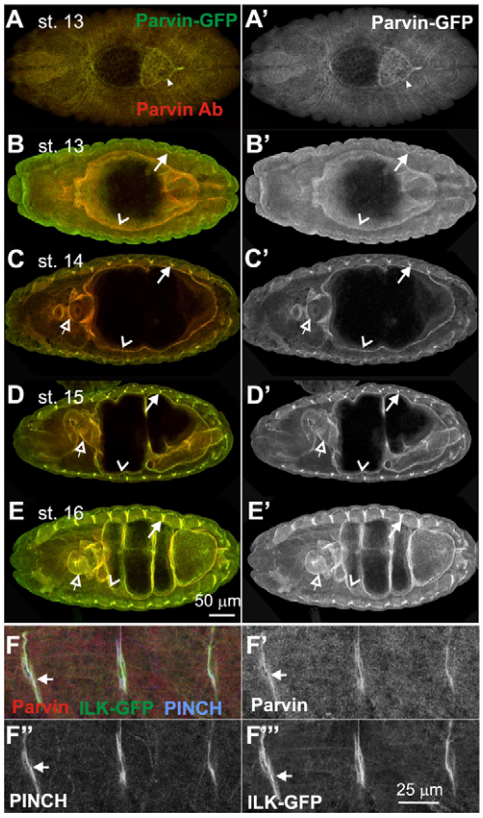

Fig. 2. Parvin is localized at sites of integrin adhesion during embryogenesis. (**A–E′**) Confocal optical sections of embryos at the indicated developmental stages showing visualization of parvin by anti-parvin antiserum (A–E, red) and parvin–GFP (A–E, green, A′–E′, white). At stage 13 only parvin–GFP is visible at low levels at the leading edge of epidermis (arrowhead; A,A′). Expression of parvin is much stronger in the developing somatic muscles (arrow) and visceral mesoderm (open arrowhead; B,B′). At later developmental stages parvin is strongly expressed in the somatic muscles and progressively accumulates at the MASs (arrow), with high expression also in visceral mesoderm (open arrowhead) and pharyngeal muscles (open arrow; C–E). Parvin is strongly colocalized with ILK–GFP at MASs (arrows). (**F–F′′′**) All components of the IPP complex are colocalized at the MASs (arrow) in the late embryo: Parvin (red), ILK–GFP (green), PINCH (blue).

parvin antiserum. Parvin–GFP was expressed at low levels in the leading edge of epidermal cells during dorsal closure at embryonic stage 13 (Fig. 2A,A′). In later developmental stages the accumulation of parvin was increased mainly in the mesoderm-derived tissues including pharyngeal, visceral and somatic muscles, with colocalization of parvin–GFP and endogenous protein (Fig. 2B–E). High amounts of parvin that progressively increased from stage 14 onwards were detected at muscle attachment sites (MASs; Fig. 2C–E). In late embryonic stages just before hatching, increased parvin accumulation was observed at the tips of muscle myosin filaments at MASs (supplementary material Fig. S3). Staining of ILK–GFP-expressing embryos with parvin and PINCH antibodies revealed that parvin strongly colocalized with both ILK and PINCH at MASs (Fig. 2F).

Generation of parvin loss-of-function alleles

To investigate the function of parvin in *Drosophila* development, we generated specific parvin deletion mutants using the EY03677 P-element line which carries a unique insertion within the 5′UTR of exon 1, 75 bp upstream of the translation start of the protein (Fig. 1B). Homozygous females and hemizygous males carrying this insertion are both viable. Upon imprecise excision we obtained 110 lethal lines that were rescued to adult viability by the 7.2 kb, but not the 3.5 kb genomic construct of parvin–GFP (Fig. 1B). We focused on two excision lines, $parvin^{251}$ and $parvin^{694}$, harboring deletions only within the parvin locus, whereas the four adjacent upstream genes remained intact (Fig. 1B). The $parvin^{251}$ line results in the elimination of the first 89 amino acids of parvin, whereas $parvin^{694}$ removes almost the entire coding sequence of the parvin locus, strongly suggesting that it is a null allele (Fig. 1B). As predicted, no detectable protein was observed by western blot for either deletion allele (Fig. 1C). To ensure that deletions in the parvin gene rather than lethal mutations in the upstream genes were being rescued by the 7.2 kb genomic rescue construct, we generated transgenic lines expressing either UAS::parvin or UAS::parvin–GFP. Lines expressing high levels of parvin in muscles or in epithelial cells induced apoptosis and lethality (Chountala, M., Vakaloglou, K. M. and Zervas, C. G.; unpublished data). However, we recovered a few lines with relatively moderate parvin expression and no dominant negative effects (Fig. 1D; supplementary material Fig. S4). These UAS::parvin lines, driven by *24BGal4*, which is known to be sufficient to rescue the *ilk* mutants (Zervas et al., 2001), resulted in almost complete rescue of the embryonic lethality of parvin deletion mutants to adult viability, with 90% of the expected adult flies recovered. However, the rescued adult flies had blisters in both wings, most likely due to insufficient expression of *24BGal4* in the wing pouch (Zervas et al., 2001). Based on these results, we concluded that both deletion lines $parvin^{694}$ and $parvin^{251}$ did not affect other essential genes, and were therefore specific alleles of *Drosophila parvin*.

Parvin functions together with ILK and PINCH in the maintenance of the integrin–actin link

The firm attachment of muscles to epidermis is abolished in integrin and integrin-associated protein mutants, exhibiting a characteristic phenotype of detached muscles and providing an excellent in vivo model system to evaluate the contribution of each component to the integrin adhesome (Narasimha and Brown, 2005).

Recently, a UAS::RNAi construct directed to parvin resulted in an integrin-like phenotype and caused larval lethality upon knockdown of the protein in muscle tissue (Langer et al., 2010). However, the lack of genetic mutants for parvin gene precluded thorough in vivo functional analysis. Here we used our parvin deletion alleles to further characterize the developmental defects associated with loss of parvin function. Both excision lines $parvin^{694}$ and $parvin^{251}$ were late embryonic lethal, indicating that parvin is required for the completion of embryogenesis. Because *ilk* and *pinch* mutants were lethal at the same developmental stage, we hypothesized that parvin could also play an essential role in the molecular machinery mediating the integrin–actin link at MASs.

We probed late embryos with Rhodamine-labeled phalloidin to visualize the organization of filamentous actin. In wild-type embryos at early stage 17, actin filaments were arranged within the muscle cells and enriched at MASs (Fig. 3A; supplementary material Fig. S5). In either $parvin^{694}$ or $parvin^{251}$ embryos,

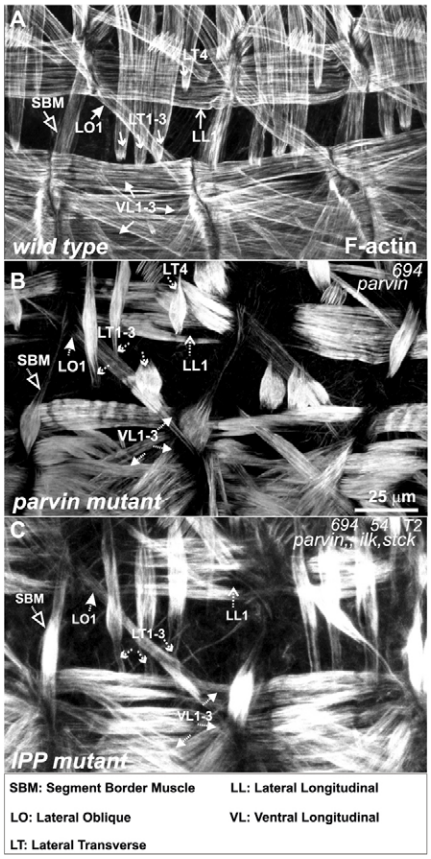

Fig. 3. Loss of parvin or function of the entire IPP complex in the embryo causes muscle detachment. Rhodamine-labeled phalloidin staining in late stage embryos to visualize F-actin. (**A**) Muscles from wild-type embryo (arrows) compared with (**B**) *parvin*^{694} mutant embryo or (**C**) *parvin*^{694}*;;ilk*^{54}*, stck*^{T2} triple mutant that display actin clumps (dashed arrows) detached from the muscle attachment sites.

F-actin was pulled away from the MASs resulting in a phenotype reminiscent of the ILK and PINCH loss of function mutants (Fig. 3B; supplementary material Fig. S5) (Clark et al., 2003; Zervas et al., 2001). We generated the first animal model containing mutations for all three genes encoding the IPP-complex proteins. The loss of function phenotype in the triple mutant was identical to the single mutants, clearly indicating that IPP-complex proteins work together to facilitate the stable linkage of actin to the integrin-containing junctions at the MASs of the *Drosophila* embryo (Fig. 3C; supplementary material Fig. S5).

Parvin stability and recruitment at MASs depends on ILK

We recently showed that ILK is essential for PINCH stability and determines its subcellular localization at MASs, although PINCH is not required for ILK recruitment (Zervas et al., 2011). Here we extended these studies to the third member of the IPP complex, parvin. We monitored recruitment of parvin–GFP expressed by its endogenous regulatory elements (7.2 kb construct) to MASs in live embryos. Whereas parvin–GFP was localized tightly at the MASs in wild-type embryos (Fig. 4A), its accumulation was completely abolished in *ilk* mutants (Fig. 4B). By contrast, PINCH has only a moderate effect on parvin protein localization as demonstrated by the partial reduction of parvin–GFP at MASs in *pinch* mutants (Fig. 4C). Interestingly, the localization of parvin–GFP at MASs in *pinch* mutants was fully restored by higher levels of ILK expressed from a UAS::ILK construct with *mef2Gal4* (Fig. 4D). Real-time qPCR data showed a similar moderate reduction (25%) on the amount of parvin mRNA in both *ilk* and *pinch* mutants (supplementary material Fig. S6). However, western blots of embryo lysates confirmed that parvin protein levels are differentially affected (Fig. 4E). Therefore the reduction on the mRNA levels alone can not account for the different effect on protein levels and an additional ILK role in controlling parvin protein stability is plausible.

Mammalian α-parvin has been proposed to bind to filamentous actin, but we were unable to observe such an association in the muscles of live embryos expressing parvin–GFP and actin5C–mRFP (Fig. 4F,F′,F′′). By contrast, a positive control consisting of the truncated form of the CH-domain-containing *Drosophila* protein spectraplakin Short stop fused to GFP (GFP–CHShot) colocalized completely with F-actin (Fig. 4G,G′) (Röper et al., 2002). Thus parvin does not appear to have a high affinity for F-actin in muscles. We used the UAS::parvin–GFP lines with *mef2Gal4* to overexpress parvin–GFP in muscles. In wild-type embryos only minimal levels of overexpressed parvin–GFP were recruited at MASs, with the bulk of the protein remaining in the cytoplasm (Fig. 4H,H′). Even at high expression levels, in *ilk* mutant embryos parvin–GFP was not enriched at MASs (Fig. 4I,I′). Thus, ILK clearly controls not only the stability of parvin but also its recruitment to MASs. By contrast, in *pinch* mutant embryos we found recruitment of parvin–GFP to MASs similar to the wild type (Fig. 4J,J′).

The decisive role of ILK in recruiting parvin was also evident later in development. In third instar larvae, continuous expression of the UAS::parvin–GFP transgene resulted in abundant accumulation of chimeric protein in the muscle cytoplasm with no enrichment at MASs (Fig. 4K,Q). Coexpression of an untagged UAS::ILK transgene resulted in a massive shift of parvin–GFP recruitment from the cytoplasm to MASs, strongly indicating that ILK is necessary and sufficient for subcellular localization of parvin (Fig. 4L,Q). Moreover, coexpression of ILK completely rescued the parvin-induced dominant lethality that we observed in the high-expressing lines, further supporting the view that ILK controls parvin function. By contrast, coexpression of either paxillin or PINCH was not sufficient to promote recruitment of parvin–GFP at MASs (Fig. 4M,N,Q).

Recruitment was used to assay parvin association with ILK. The interaction motifs involved in the association of ILK kinase domain and parvin CH2 domain have been thoroughly analyzed and precise amino acids involved in the interaction have been identified (Fukuda et al., 2009). We tested the effect of two point mutations of ILK that have been shown to completely rescue the *ilk* mutant phenotype to adult viability: (1) E356K located near the kinase binding interface with the CH2 domain and (2) F436A located at the distal part of the kinase domain far away from the interaction interface (Zervas et al., 2001; Zervas et al., 2011). Surprisingly, both mutations strongly impaired the efficient recruitment of high levels of parvin–GFP from the cytoplasm to MASs, without affecting recruitment to Z-discs (Fig. 4O–Q). By contrast, in *ilk* mutants rescued by transgenes containing either the E356K (Fig. 4R) or F436A (data not shown) parvin recruitment at MASs was normal. Thus, the contribution of E356K and F436A mutations became apparent only when

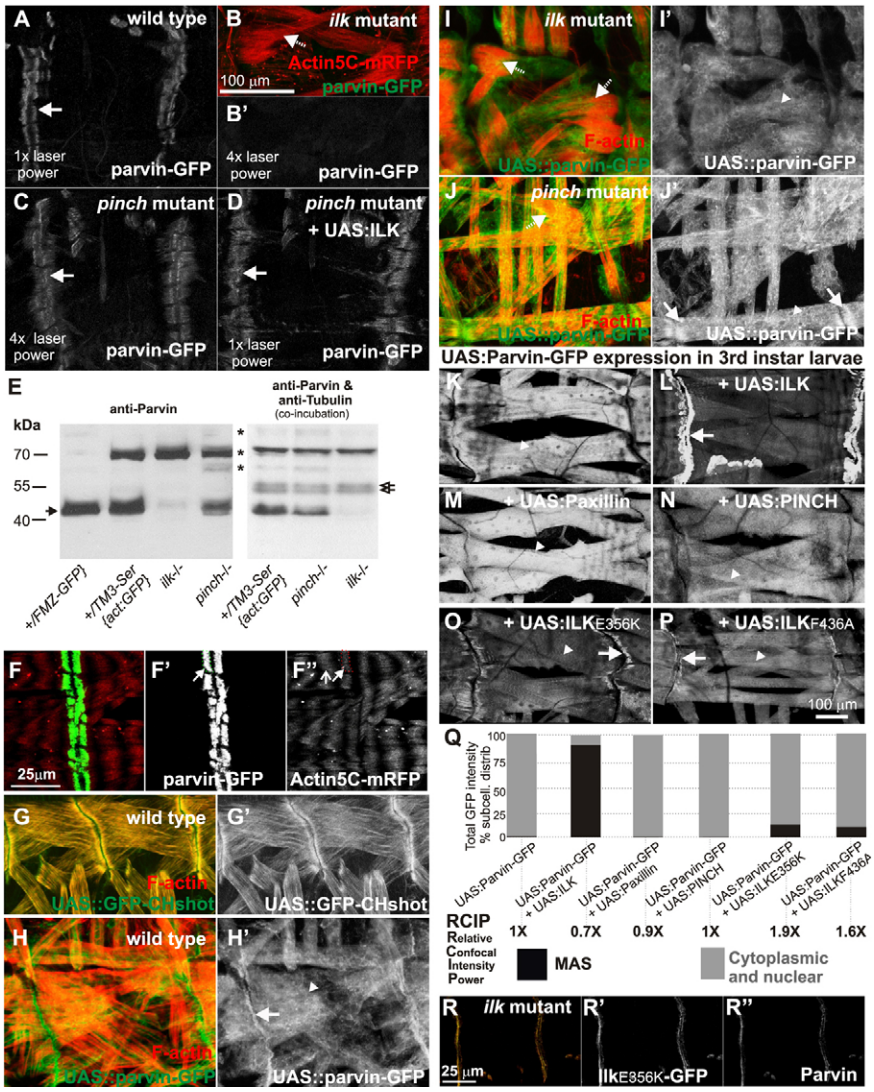

Fig. 4. ILK levels control parvin stability and recruitment at MASs. (**A–D**) Dorsal oblique muscles of late stage living embryos expressing parvin–GFP. (**E**) Western blot showing parvin (left panel) or both parvin and tubulin (right panel). Asterisks (*), indicate non-specific bands that appeared in a genotype-dependent manner (compare FMZ–GFP with +/TM3-Ser{act:GFP}). The closed arrow indicates the endogenous parvin and the open arrows the tubulin doublet band. (**F**) MASs at dorsal oblique muscles from a late embryo expressing parvin–GFP (green, **F′**) and actin5C–mRFP (red, F′′). (**G–J**) Somatic muscles of late embryos expressing GFP–CHShot (green, G) or high levels of parvin–GFP (green, H) and F-actin visualized with Rhodamine-labeled phalloidin (red) in wild type (G,H), *ilk* mutants (I) or *pinch* mutants (J). (**K–P**) Third instar larvae muscles expressing parvin–GFP with *mef2Gal4* (K) together with UAS::ILK (L), UAS::Paxillin (M), UAS::PINCH (N), UAS::ILK^{E356K} (O) and UAS::ILK^{F436A} (P). In A–D and F–P, arrows denote MASs, dashed arrows indicate detached actin filaments and arrowheads indicate cytoplasm. (**Q**) Quantification of the fluorescence intensity distribution at MASs compared with that in the cytoplasm. The relative confocal intensity power (RCIP) used for the acquisition of each depicted image is given. (**R**) Dorsal oblique muscles with normal parvin levels (red, R′′) in an *ilk* mutant embryo rescued by the genomic construct of ILK–GFP (green, R′) carrying the E356K mutation.

increased levels of parvin were present and high binding affinity to ILK was required for efficient accumulation at MASs.

Parvin domains required for localization at MASs

To identify which parvin domains are required for protein localization and function, we engineered deletions of UAS::parvin–GFP and analyzed their expression (driven by *mef2Gal4*) and localization in established transgenic lines (supplementary material Fig. S4). As before (Fig. 4), overexpression of parvin–GFP in wild-type embryos resulted in cytoplasmic accumulation of the majority of the protein with only 25% at MASs (Fig. 5A,J). Deletion of either the N-terminus (UAS::parvin^{CH1CH2}–GFP) or the CH1 domain (UAS::parvin$^{\Delta CH1}$–GFP) did not significantly affect distribution, suggesting that these two regions are not essential for targeting parvin to MASs (Fig. 5B,C). Both truncated parvin forms actually showed a small increase at MASs to about 30% of total protein expressed (Fig. 5J). However, removal of the CH2 domain (UAS::parvin$^{\Delta CH2}$–GFP) resulted in accumulation in the cytoplasm and around the nuclei instead of at MASs (Fig. 5D,J). To avoid saturation by overexpressing UAS::parvin$^{\Delta CH2}$–GFP in the muscles, we expressed the same deletion construct from the endogenous regulatory elements (parvin$^{\Delta CH2}$–GFP). Several transgenic lines expressing truncated parvin at either low or high levels showed no enrichment at MASs (supplementary material Fig. S7). We concluded that the available binding sites for parvin at MASs are limited and that parvin subcellular localization depends on the presence of the CH2 domain. Interestingly, CH2–GFP alone (UAS::parvin^{CH2}–GFP) was poorly expressed in late embryos and less than 25% of the expressed protein was located at MASs (Fig. 5E,J). Thus, although the CH2 domain is sufficient for localization, it is unstable. CH1–GFP (UAS::parvin^{CH1}–GFP) was harder to detect and therefore even less stable (Fig. 5F,J). By contrast, the N-terminus of parvin (UAS::parvin^{Nter}–GFP) was stable, but completely lacked the ability to localize to MASs (Fig. 5G,J). Either the N-terminus or the linker region conferred stability to the CH1 domain (UAS::parvin^{NCH1}–GFP and UAS::parvin^{CH1L}–GFP; Fig. 5H,I). Coexpression of the untagged N-terminal region (UAS::N-terminus), as verified by anti-parvin antibody staining (supplementary material Fig. S8), improved neither the stability of the CH1 domain (UAS::parvin^{CH1}–GFP) nor its recruitment to MASs, indicating that the two domains needed to be present in the same molecule, rather than in trans (data not shown).

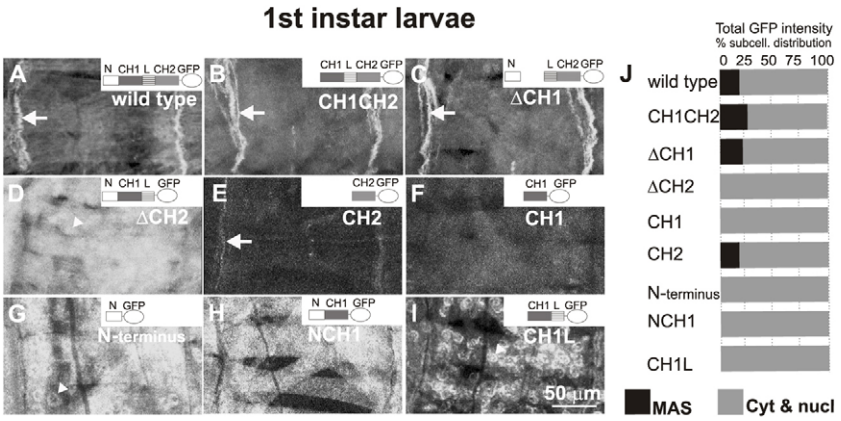

Fig. 5. Localization properties of overexpressed mutant forms of parvin–GFP in newly hatched first instar larvae. (**A–I**) Projections of confocal sections of lateral longitudinal muscles from larvae expressing wild-type and mutant forms of UAS::parvin–GFP driven by *mef2Gal4*. Arrows, parvin–GFP at MASs; arrowheads, perinuclear regions. (**J**) Quantification of fluorescence intensity distribution at MASs compared to that in the cytoplasm.

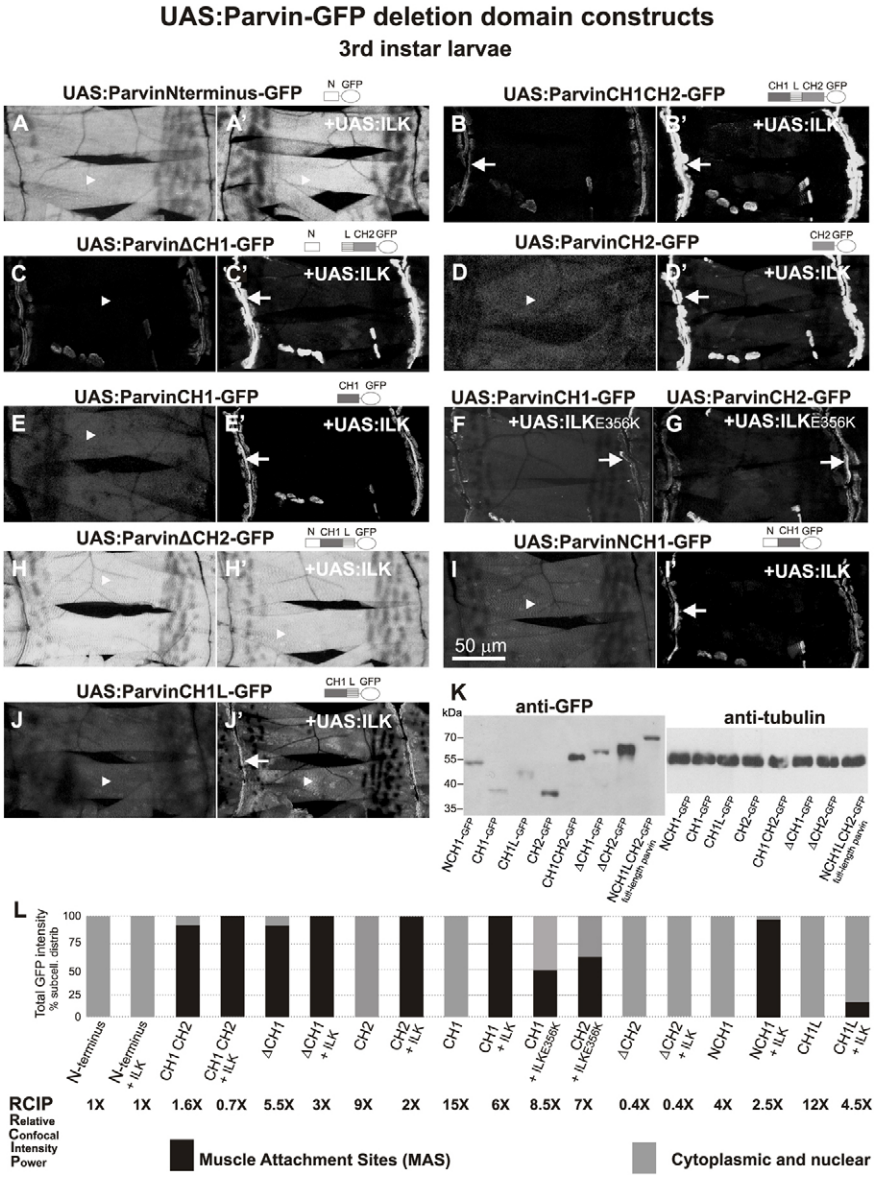

Fig. 6. MAS recruitment of overexpressed mutant forms of parvin–GFP upon coexpression with ILK in third instar larvae. (**A–J**) Projections of confocal sections of dorsal oblique muscles from third instar larvae expressing mutant forms of UAS::parvin–GFP alone (A–E, H–J) or with wild-type or mutant UAS::ILK (A′–E′,H′–J′,F–G) driven by *mef2Gal4*. Arrows, parvin–GFP at MASs; arrowheads, parvin–GFP in the cytoplasm. (**K**) Western blot showing expression levels of parvin and parvin domains fused to GFP when coexpressed with ILK in first instar larvae lysates; tubulin as loading control. (**L**) Quantification of the fluorescence intensity distribution at MASs compared to cytoplasm and the RCIP used for the acquisition of each depicted image in comparison to the full-length parvin–GFP (1×; Fig. 4K).

Identification of a novel localization signal in the CH1 domain

The lack of stability of CH1–GFP and CH2–GFP precluded detailed studies of their recruitment to MASs. Because we found that ILK levels controlled the stability and amount of parvin recruited to MASs, we investigated the effect of ILK on the stability and localization of individual domains. Parvin truncated forms were expressed using *mef2Gal4*, with or without coexpression of ILK, and analyzed both by confocal microscopy in live larvae (Fig. 6A–J) and by western analysis of protein extracts (Fig. 6K). Localization of the N-terminal region remained cytoplasmic even when ILK was coexpressed (Fig. 6A,A′,L). However, truncated parvin lacking either the N-terminal region (UAS::parvin^{CH1CH2}–GFP) or the CH1 domain (UAS::parvin$^{\Delta CH1}$–GFP) showed a significant increase in GFP fluorescence when coexpressed with ILK and were able to localize at MASs (Fig. 6B,B′,C,C′). Similarly, coexpression of CH2 domain (UAS::parvin^{CH2}–GFP) with ILK enhanced its stability and resulted in its complete recruitment to MASs (Fig. 6D′,L), compared to hardly detectable expression in the absence of ILK (Fig. 6D,L). However, analysis of the CH1 domain (UAS::parvin^{CH1}–GFP) revealed a surprising result. Unlike the very low levels detected within the cytoplasm when expressed alone, coexpression of ILK considerably stabilized CH1–GFP and triggered its recruitment to MASs (Fig. 6E,E′,L). Thus we concluded that parvin contains two localization signals; one within the CH2 domain and a second novel one within the CH1 domain. Both localization signals are controlled by ILK. Coexpression of the E356K ILK mutant was less efficient at recruitment of either CH1–GFP or CH2–GFP to MASs, suggesting that the CH domains of parvin may share a similar binding site within the kinase domain of ILK (Fig. 6F,G,L). Interestingly, truncated parvin lacking only the CH2 domain (UAS::parvin$^{\Delta CH2}$–GFP) was unable to localize at MASs even when coexpressed with ILK (Fig. 6H,H′), suggesting that the localization signal in the CH1–domain is masked. We hypothesized that the N-terminus and/or linker are responsible for masking the CH1–domain localization signal. As noted previously, in first instar larvae (Fig. 5H,I), coexpression of the N-terminal region or the linker together with the CH1 domain in the same molecule (UAS::parvin^{NCH1}–GFP and UAS::parvin^{CH1L}–GFP) resulted in its stabilization and localization in the cytoplasm. However, only NCH1–GFP was efficiently recruited to MASs upon coexpression of ILK, whereas CH1L–GFP showed partial recruitment with almost 85% of the chimeric protein remaining cytoplasmic (Fig. 6I′,J′,L). These results indicated that the linker sequence was primarily responsible for masking the localization signal in the CH1 domain, when the CH2 domain was missing.

Functional analysis of parvin mutants

Next we explored the ability of truncated parvin proteins to functionally rescue the parvin mutant, using several transgenic lines to control for variable expression (supplementary material

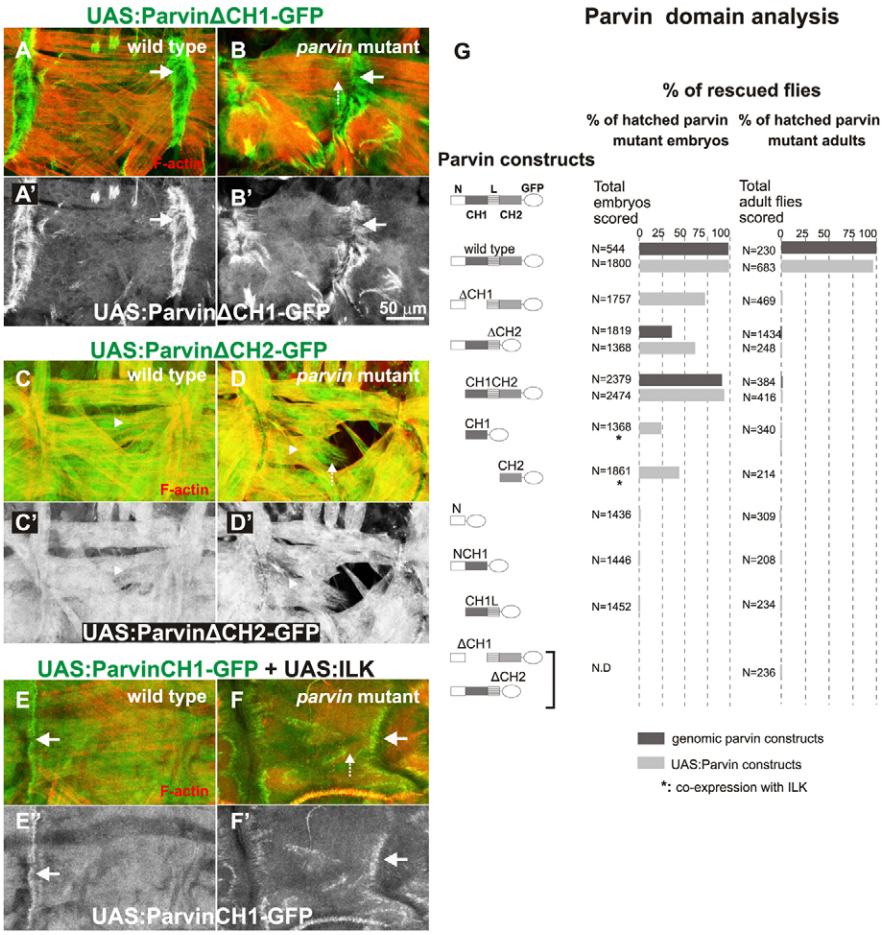

Fig. 7. Functional analysis of parvin domains in mediating the integrin–actin link. (**A–F**) Stacks of confocal sections of muscles from stage 17 wild-type embryos (A,C,E) or *parvin* mutant embryos expressing truncated parvin forms overexpressed using *24BGal4* (B,D,F). Parvin–GFP, green; phalloidin-stained F-actin, red. Arrows, parvin–GFP at MASs; dashed arrows, detached muscles; arrowheads, cytoplasm. (**G**) Rescue efficiency of all constructs tested.

Fig. S4). Unlike full length parvin, none of the domain deletion mutants overexpressed by *mef2Gal4* caused any dominant negative effects.

Expression of parvin without the CH1 domain (UAS::parvin$^{\Delta CH1}$–GFP) significantly rescued embryonic lethality of parvin mutants (up to 75% of mutant embryos hatched to first instar larvae) but the larvae died during the first and second instar stage, exhibiting a muscle detachment phenotype similar to embryos (Fig. 7A,B,G). Thus CH1 is essential for parvin function mainly at the early larval stages that coincide with enhanced muscle contractility. Next we tested the effect of deleting the CH2 domain. Expression from either the endogenous parvin regulatory elements or from the UAS promoter partially rescued embryonic lethality, but all rescued larvae died soon after hatching with muscle adhesion defects (Fig. 7C,D,G), indicating that the CH2 domain is required for proper embryonic development. Interestingly, we found that expression of truncated parvin lacking the N-terminal region (parvin^{CH1CH2}–GFP) rescued both embryogenesis and larval development, but development of the mutant flies was arrested at the pupae stage (Fig. 7G). Thus, in *Drosophila*, the N-terminal region also participates in molecular interactions essential for later developmental stages.

Given that the CH1 domain is necessary for parvin function and is sufficiently recruited at MASs when co-expressed with ILK, we examined whether co-overexpression of CH1–GFP and ILK could rescue the parvin mutant. We found that although the novel localization signal of CH1–GFP was capable of mediating its localization to MASs in the absence of endogenous parvin (Fig. 7E,F), rescue activity was poor (Fig. 7G). The rescue activity of the CH2–GFP domain stabilized by coexpression with ILK was better because almost 50% of the embryos hatched before dying as first instar larvae (Fig. 7G). Despite stable expression, parvin mutants were not rescued by any other truncated parvin form containing either the N-terminus alone (UAS::parvin^{N}–GFP), the N-terminal region and CH1 domain (UAS::parvin^{NCH1}–GFP) or the CH1 domain and linker sequence (UAS::parvin^{CH1L}–GFP). Because we found that all domains are required for parvin function, we next tested whether they needed to be present in the same molecule. Coexpression of UAS:parvin$^{\Delta CH1}$–GFP and UAS:parvin$^{\Delta CH2}$–GFP did not improve rescue ability, but instead provided zero rescue (Fig. 7G). Thus, all domains of parvin need to be present in the same molecule, supporting its structural role in connecting at least two other proteins together at MASs.

ILK, Paxillin, PINCH and α-actinin do not require parvin localization at MASs

Given the high accumulation of parvin at MASs and the identical phenotype of *parvin*, *ilk* and *pinch* mutants, we asked whether parvin is required for subcellular localization of its interacting proteins ILK, paxillin, α-actinin and PINCH (Nikolopoulos and Turner, 2000; Yamaji et al., 2004). We found identical recruitment of these proteins in parvin mutants and wild-type embryos (supplementary material Fig. S9). The localization at MASs of another four proteins that associate with the integrin adhesion machinery, zyxin, tensin, zasp52 and the activated form of FAK, was also unchanged in parvin mutants (supplementary material Fig. S10). These results strongly suggest that parvin does not participate in the assembly of the integrin–actin linker complex at MASs but rather functions to strengthen the integrin–actin link.

Stability and localization of parvin/ILK/PINCH are interdependent in wing epithelium

To detail the in vivo role of parvin function in the developing organism, we examined its expression and function in the wing epithelium, another well established model of integrin-mediated adhesion in *Drosophila*, where integrin loss-of-function mutations result in the formation of wing blisters (Bökel and Brown, 2002). Integrins are organized in focal contact-like structures at the basal side of the wing epithelium where they mediate the adhesion of the two opposing epithelial layers (Brown et al., 2002). We found that parvin–GFP accumulated in

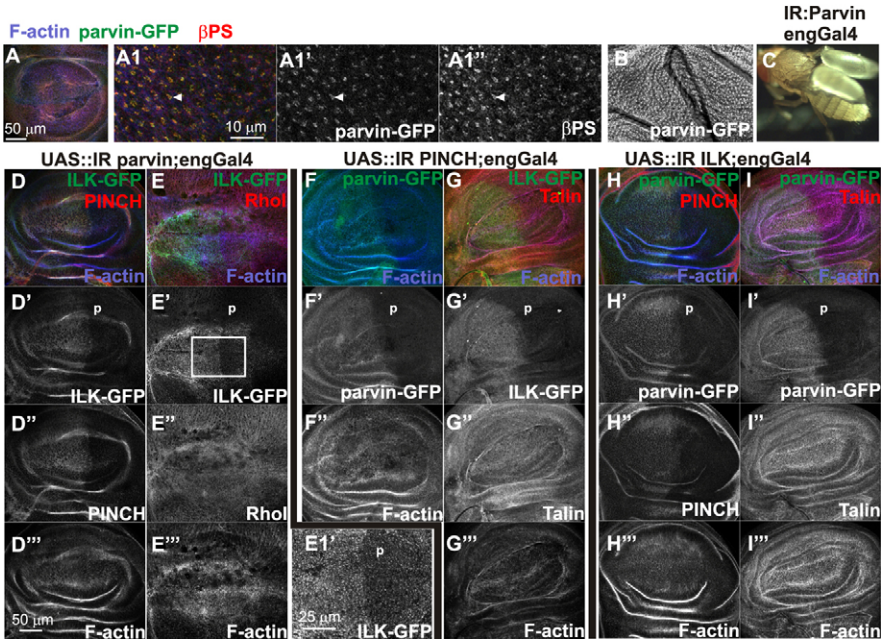

Fig. 8. Parvin expression and function at the basal side of the wing epithelium. (**A**, magnified in **A1**) parvin–GFP (green in A1, white in **A1′**) colocalizes with βPS (red in A1, white in **A1′′**) at the focal-contact-like structures at the basal side of the wing epithelium of third instar larvae. F-actin visualized with Rhodamine–phalloidin (blue). (**B**) Parvin–GFP is also expressed later in development and localizes basally in the wing epithelium of a pharate adult. (**C**) Adult fly with blisters in both wings upon knockdown of parvin with *engrailedGal4*. (**D–I′′′**) Mutual dependence of IPP-complex members for stability and localization, in the epithelium of an imaginal wing disc from a third instar larva. Each IPP-complex component was knocked down in the posterior compartment (p) of the wing disc with an *engrailedGal4* UAS::IR construct. Tissue integrity observed by F-actin (blue) and RhoI (red). (D,E) Knockdown of parvin results in significant reduction of ILK-GFP posteriorly (D′,E′ and magnified insert E1′) and PINCH (D′′). (F,G) Knockdown of PINCH results in the elimination of parvin–GFP (F′) and ILK–GFP (G′). (H,I) Knockdown of ILK results in the elimination of parvin–GFP (H′,I′) and PINCH (H′′). Knockdown of PINCH or ILK did not affect talin (G′′,I′′).

the focal contact-like structures stained with antibodies against βPS integrin in larval imaginal discs (Fig. 8A,A1). Later in development of the pupae wing, parvin–GFP also tightly localized at the basal side of the epithelium (Fig. 8A,A1,B).

To study parvin function in wing development, we expressed UAS::RNAi constructs targeting either part of parvin exon 4 (VDRC collection, Fig. 1B), or the entire exon 4 (our own construct, Fig. 1B) in the posterior compartment of the wing using *engGal4*. All adult flies had blisters in both wings (Fig. 8C). Taken together, these data suggest that parvin functions in combination with integrins in the developing wing epithelium.

To further analyze the functional relationship of IPP-complex components in terms of stability and recruitment to focal contact-like structures in the wing, we used RNAi-induced knockdown of each component and examined expression of the remaining two (Dietzl et al., 2007). We found a similar mode of interdependency of the IPP-complex components as in mammalian cells. Upon knockdown of parvin specifically in the posterior compartment, both ILK–GFP and PINCH were largely decreased, although RhoI levels remained unaffected (Fig. 8D,E). Similarly, knockdown of either PINCH or ILK resulted in reduced expression of parvin–GFP and ILK–GFP (Fig. 8F,G), or parvin–GFP and PINCH (Fig. 8H), respectively, whereas talin levels remained unchanged (Fig. 8I). Thus unlike at MASs, in the wing epithelium the endogenous protein levels of ILK, PINCH and parvin are mutually dependent and directly correlated with the assembly of the IPP complex.

Discussion

In this study, we established the essential role of parvin in integrin-mediated adhesion and demonstrated that parvin participates together with ILK and PINCH in the maintenance of the integrin–actin link in vivo. These conclusions are supported by: (1) the identical muscle phenotype of parvin mutants to mutants of ILK, PINCH and the triple mutant; (2) colocalization of all three proteins at sites of integrin adhesion; (3) the fact that ILK is necessary and sufficient for parvin stability and recruitment to MASs; (4) the suppression of dominant negative effects of overexpressed parvin within muscle by ILK; and (5) interdependence of all three IPP-complex components for their stability and subcellular localization at the basal side of wing epithelia, unlike the central role of ILK in IPP-complex assembly at the embryonic MASs. Our results suggest that depending on the cell context, discrete molecular events coordinate the assembly of adhesion complexes into functional attachment structures (Fig. 9).

The IPP complex functions as a unit at MASs in the *Drosophila* embryo

We generated parvin mutants to complete the functional characterization of the entire IPP complex in *Drosophila* development. *parvin* null mutants shared similar phenotypic abnormalities with ILK and PINCH mutants as well as the integrin hypomorphic mutations described previously, including muscle defects due to actin filament retraction from the muscle ends in the late embryo (Clark et al., 2003; Devenport et al., 2007; Zervas et al., 2001). The muscle defects and lethality associated with parvin mutants was completely rescued by moderate expression of a wild-type parvin transgene mainly in somatic muscles and tendon cells, indicating that parvin has

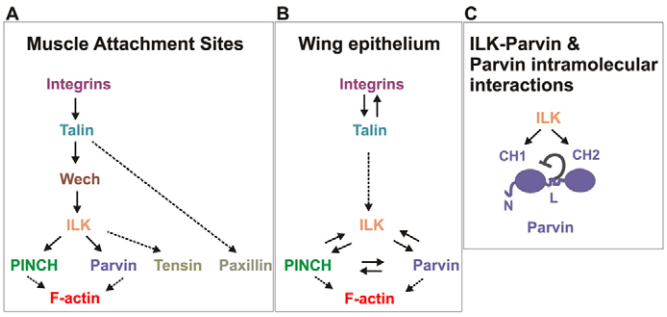

Fig. 9. Genetic hierarchy of integrin–actin linker complex assembly at MASs and in wing epithelium. (**A**) At MASs, assembly of the integrin–actin linker complex follows a linear pathway of genetic interactions. IPP-complex assembly depends on ILK and there is no interdependency between parvin and PINCH. (**B**) In the wing epithelium the genetic hierarchy can be classified at two levels: Integrins and talin are mutually dependent and both are required for IPP-complex stability. All proteins of the IPP complex are mutually dependent. (**C**) Mode of parvin interactions with ILK.

essential functions in these tissues. We generated the first in vivo triple null mutant in an animal for all proteins that comprise the IPP complex. The identical loss-of-function phenotype at muscles in the triple versus single mutants strongly suggests that these three proteins work together as a complex by reinforcing the integrin–actin link at MASs in the *Drosophila* embryo. Although loss of parvin function at the muscles causes defective adhesion, high levels of parvin is also detrimental for the developing organism, suggesting that unlike overexpression of other IPP-complex members, the amount and subcellular localization of parvin needs to be tightly regulated.

Parvin recruitment at MASs by ILK

parvin recruitment at MASs appears to depend exclusively on its interaction with ILK. In the absence of ILK, endogenous parvin protein levels are drastically reduced as previously reported (Lin et al., 2003; Wu, 2004). Although endogenous parvin protein levels also decrease in the absence of PINCH, most likely due to moderate reduction of the parvin mRNA levels, this can be completely rescued by coexpression of ILK. Previously, we showed that removal of PINCH does not affect the levels of a genomic ILK–GFP transgene. However, its effect on endogenous ILK levels remains undetermined due to the lack of a specific antibody against *Drosophila* ILK. Therefore, even a slight reduction of endogenous ILK levels in *pinch* mutants can not be excluded, providing an alternative explanation for both the moderate reduction of parvin and its complete restoration upon ILK overexpression. Overexpressed parvin in muscle cells remains in the cytoplasm, suggesting that the number of available binding sites for parvin at MASs is limited. However, simultaneous overexpression of parvin and ILK results in accumulation of parvin at MASs, indicating that ILK is necessary and sufficient for subcellular localization of parvin. High levels of cytoplasmic uncomplexed parvin in muscle cells induce dominant lethality, which is reversed upon coexpression of ILK. Previous studies in cells have shown that an imbalance in the amount of α- and β-parvin complexed with ILK induces apoptosis. Taken together these results suggest that the stoichiometry of ILK and parvin is crucial (Zhang et al., 2004). Indeed, in *Drosophila* embryos and S2R^{+} cells, all components of

the IPP complex are co-purified in stoichiometric amounts (Kadrmas et al., 2004).

Parvin is known to be recruited to sites of integrin adhesion by direct interaction of its CH2 domain with the kinase domain of ILK (Fukuda et al., 2009). Here we also show that the CH2 domain of *Drosophila* parvin is sufficient for localization to MASs. In addition, we uncovered a novel ability of the parvin CH1 domain to localize at integrin junctions (Fig. 9C). The close correlation between the levels of ILK and the stability and localization of the CH1 domain strongly suggest their direct interaction. Based on the similar negative effect of the E356K mutation of ILK on the recruitment of each CH domain, we predict that they bind to the same site within the kinase domain of ILK, although with different affinity. An alternative explanation that we favor less is the existence of a factor-X that recruits the CH1 domain at MASs, whereas ILK mediates factor-X recruitment. One candidate could be the fly homolog of αPIX, *dPix*, which is localized at MASs and binds to the CH1 domain of β-parvin in mammalian cells (Mishima et al., 2004; Parnas et al., 2001).

Our data suggests that the CH1 domain localization signal is masked by the linker region. Although we did not provide direct biochemical evidence supporting such an intramolecular interaction, a similar interaction has been reported in filamin, another CH-domain-containing protein (Nakamura et al., 2005). Given the strong possibility that both CH domains of parvin interact with ILK, the linker might function as a regulatory module ensuring that only high affinity interactions between parvin and ILK occur, thus controlling recruitment of parvin at MASs. The functional significance of parvin CH1-domain interaction with ILK requires further investigation involving the identification of specific mutations within the CH1 domain that could disrupt the binding on ILK.

Parvin colocalizes with F-actin only at sites of integrin adhesion

Proteins containing tandem CH domains possess the ability to bind to filamentous actin (Gimona et al., 2002). Mammalian parvins show a differential ability to bind to F-actin. Although human α-parvin binds to actin filaments, β-parvin does not, despite 73% sequence identity (Sepulveda and Wu, 2006). In mammalian cells, both α and β-parvin are largely associated with focal adhesions rather than the actin cytoskeletal filaments (Nikolopoulos and Turner, 2000; Olski et al., 2001; Yamaji et al., 2001). In the living fly embryo, we found that parvin–GFP expressed from its own promoter was similarly not colocalized with F-actin in the muscle cells, but instead accumulated heavily at MASs. By contrast, the two CH domains of Short stop colocalized with filamentous actin (Röper et al., 2002). These findings reflect differences in affinity for actin as supported by *in vitro* dissociation constants (ShotCH 0.022 μM and α-parvin 8 μM) (Lee and Kolodziej, 2002; Olski et al., 2001). Thus, within muscles parvin does not appear to have sufficient actin binding activity to co-distribute with actin filaments. Given that several proteins are known to bind to both CH domains in regions overlapping the putative actin binding sites, the role of parvin as an actin-binding protein In vivo is questionable. Hence, interaction of the CH domains with F-actin appears to be either less favored or to occur only in a highly regulated manner at sites of integrin adhesion (Sepulveda and Wu, 2006).

Insights into the functional requirement of parvin domains

Studies of mammalian parvins have suggested possible biochemical functions for *Drosophila* parvin (Kimura et al., 2010; LaLonde et al., 2005; LaLonde et al., 2006; Mishima et al., 2004; Rosenberger et al., 2003). To gain further insight into the mechanisms by which parvin functions in integrin-mediated adhesion, we assessed the functional requirement of each protein domain. We demonstrated that both the CH1 and CH2 domains are essential to strengthen the integrin-actin link and their importance coincides with their capacity to mediate an interaction with ILK that is responsible for their individual localization. Moreover, both CH domains are required in the same molecule. Hence, it is likely that these parvin domains link ILK and other proteins together to maintain the integrin-actin link. We also found that the less well conserved N-terminal region of parvin is not essential for integrin-mediated adhesion at MASs, similar to *pat-6* N-terminal domain in *C. elegans* (Lin et al., 2003). However, later in development the N-terminus becomes indispensable, suggesting a different set of essential molecular interactions for parvin depending on the developmental context.

Mutually dependent interactions underlie IPP-complex stability in wing epithelium

In mammalian cells all three proteins of the IPP complex are mutually dependent for their stability and recruitment at sites of integrin adhesion (Zhang et al., 2002). However, genetic studies both in *C. elegans* and *Drosophila* have shown that in muscle cells ILK behaves as a master component for complex assembly (Lin et al., 2003; Zervas et al., 2011). Several studies have pointed out that the two well established models for stable adhesion in *Drosophila*, MASs and the basal side of the wing epithelium, exhibit molecular differences in assembly properties of the integrin adhesion complex, as well as differential sensitivity in genetically induced perturbations (Delon and Brown, 2007). In agreement with these studies, we showed that in the wing epithelium the hierarchy of genetic interactions among the IPP-complex members differs and that, like in mammalian cells (Zhang et al., 2002), the three proteins are interdependent for their stability and subcellular localization (Fig. 9). This finding highlights the existence of diverse molecular strategies capable of mediating distinct adhesion properties in the developing organism and therefore underlines the importance of In vivo analysis of the same molecular machine of integrin adhesion junctions in various morphogenetic processes.

Materials and Methods

parvin mutagenesis and *Drosophila* genetics

parvin deletion alleles $parvin^{251}$ and $parvin^{694}$ were generated during imprecise excision of the P-element *EY03677* (BL-15669). Rescue was assayed by crossing parvin rescue constructs with each of the lethal lines and looking for males without *Bar*. Excision alleles were mapped by PCR followed by DNA sequencing. UAS transgenes with appropriate *GAL4* drivers (FlyBase) were used to assay rescue of *parvin* mutant alleles.

The following fly stocks were described previously: ilk^{54}, $stck^{T2}$, UAS::ILK^{F436A}, UAS::ILK^{E356K}, UAS::paxillin, UAS::PINCH (Zervas et al., 2011), *ilk-gfp* (Zervas et al., 2001), *tensin-gfp* (Torgler et al., 2004). UAS::Zyxin-ChRFP (BL-28875), UAS::Actin5C-mRFP (BL-24779) and Zasp52-GFP (BL-6838) were obtained from Bloomington. The protein GFP trap for α-actinin-GFP (CC01961) was obtained from A. Spradling (Buszczak et al., 2007) and the UAS:IR stocks from the VDRC collection (Dietzl et al., 2007).

Molecular biology of parvin transgenes

The BAC clone 48P17 was digested with *Not*I and *Xba*I and the 7.2 kb genomic fragment was subcloned into pBluescript. The 3.5 kb fragment was subcloned with *Xho*I and *Xba*I. mGFP6 was derived from the *ilk-GFP* construct, cloned in-frame with the parvin coding region including a small four-serine linker and finally subcloned into the P-element transformation vector pWhiteRabbit (Zervas et al., 2001). A full-length cDNA was amplified from a 4–8 hr cDNA library using appropriate primers to construct transgenes (Brown and Kafatos, 1988). After confirmation by DNA sequencing, each transgene was subcloned into the transformation vector pUASp. Several transgenic lines were obtained following standard protocols.

qPCR in embryos

Total RNA was isolated from wild-type, *ilk* and *pinch* mutant embryos using the RNeasy kit (Qiagen). First-strand synthesis was performed using QuantiTect Reverse Transcription kit (Qiagen) following the manufacturer's instructions. SYBRGreeER qPCR SuperMix Universal (Invitrogen) was used for the amplification and detection of DNA in real-time qPCR. Experiments were performed with the ABI Prism 7000 Sequence Detection system from Applied Biosystems. Ribosomal protein L32 was used as a reference gene. Duplicates of each reaction were performed in parallel and were repeated for two independently isolated RNA samples. Primer sequences are listed in supplementary material Fig. S6.

Generation of anti-parvin antibody

We prepared a polyclonal antibody using the GST-tagged fusion protein corresponding to parvin amino acids 1–241 after cloning of the *Bam*HI–XbaI fragment of the cDNA clone GH23568 into pGEX4T2 (Pharmacia). Expression and purification of the recombinant protein was performed according to the manufacturer's recommendations. Antibody specificity was tested by western blotting and immunohistochemistry in both wild-type and parvin mutant embryos, as well as embryos expressing a UAS::parvin–GFP transgene using several *GAL4* lines.

Immunofluorescence and western blotting

Whole-mount labeling of embryos was performed as described (Zervas et al., 2011), followed by standard antibody labeling. Imaginal wing discs were dissected from third-instar larvae and fixed in phosphate buffered saline containing 4% formaldehyde for 30 min. Primary antibodies were against: parvin (rabbit polyclonal; 1:500), PINCH (rabbit polyclonal; 1:500) (Clark et al., 2003), paxillin (rabbit polyclonal; 1:500) (Chen et al., 2005), pY397-FAK (rabbit polyclonal; 1:500, Cell Signaling), MHC (myosin heavy chain) (mouse monoclonal; 1:60) (Kiehart et al., 1990), and βPS (mouse monoclonal CF.6G11; 1:10) (Brower et al., 1984). Secondary antibodies were conjugated to Alexa-Fluor-488, -568, or -633 (1:500, Molecular Probes). F-actin was detected with either Rhodamine or Alexa-Fluor-635-labeled phalloidin (R-415 and A34054, Molecular Probes). Images were obtained with a Leica SP5 confocal microscope using a 20×/0.7 or oil 63×/1.4 objective. Leica SP5 software was used for quantification. The confocal settings were adjusted to avoid pixel intensity saturation. Selected areas at MASs, nuclei or entire muscle areas were outlined in at least four different animals, the total intensity measured and plotted using Excel. Images were assembled in Photoshop 7 and labeled in Corel Draw 12. Protein lysates were prepared from late embryos or first instar larvae and analyzed by western blotting with antibodies against parvin, GFP (Molecular Probes) and tubulin (Sigma) as a loading control. Blots were then probed with horseradish peroxidase (HRP)-conjugated anti-rabbit or anti-mouse Ig secondary antibodies (Jackson Laboratories; 1:30,000) and were developed using Western Lighting Ultra Chemiluminescence Reagent (Perkin Elmer).

Acknowledgements

This study was initiated in the lab of Nick Brown at the Gurdon Institute, University of Cambridge, UK, and we appreciate his support. We also thank Stamatis Pagakis for imaging analysis suggestions, Vassiliki Kostourou for critically reading the manuscript, Ioannis Serafimidis for help in qPCR, Elpinickie Ninou for assistance in embryo stainings for Fig. 3 and supplementary material Fig. S5, and Victoria Williams for assistance in the early stages of this study. We thank Bloomington Drosophila Stock Center, VDRC (Vienna), Developmental Studies Hybridoma Bank at the University of Iowa (DSHB) and DGRC for sharing fly stocks, antibodies, and DNA plasmids, and Alan Sprandling for GFP fly traps.

Funding

This work was supported by the Greek Secretariat for Research and Technology [grant number PENED-03ED777 to C.G.Z.]; Association Française contre les Myopathies (AFM) [grant number 12641 to C.G.Z.]; and intramural funds of Biomedical Research Foundation, Academy of Athens [to C.G.Z.].

Supplementary material available online at
http://jcs.biologists.org/lookup/suppl/doi:10.1242/jcs.102384/-/DC1

References

Bökel, C. and Brown, N. H. (2002). Integrins in development: moving on, responding to, and sticking to the extracellular matrix. *Dev. Cell* **3**, 311-321.

Brower, D. L., Wilcox, M., Piovant, M., Smith, R. J. and Reger, L. A. (1984). Related cell-surface antigens expressed with positional specificity in *Drosophila* imaginal discs. *Proc. Natl. Acad. Sci. USA* **81**, 7485-7489.

Brown, N. H. and Kafatos, F. C. (1988). Functional cDNA libraries from *Drosophila* embryos. *J. Mol. Biol.* **203**, 425-437.

Brown, N. H., Gregory, S. L., Rickoll, W. L., Fessler, L. I., Prout, M., White, R. A. and Fristrom, J. W. (2002). Talin is essential for integrin function in Drosophila. *Dev. Cell* **3**, 569-579.

Buszczak, M., Paterno, S., Lighthouse, D., Bachman, J., Planck, J., Owen, S., Skora, A. D., Nystul, T. G., Ohlstein, B., Allen, A. et al. (2007). The carnegie protein trap library: a versatile tool for Drosophila developmental studies. *Genetics* **175**, 1505-1531.

Chen, G. C., Turano, B., Ruest, P. J., Hagel, M., Settleman, J. and Thomas, S. M. (2005). Regulation of Rho and Rac signaling to the actin cytoskeleton by paxillin during Drosophila development. *Mol. Cell. Biol.* **25**, 979-987.

Chu, H., Thievessen, I., Sixt, M., Lämmermann, T., Waisman, A., Braun, A., Noegel, A. A. and Fässler, R. (2006). γ-Parvin is dispensable for hematopoiesis, leukocyte trafficking, and T-cell-dependent antibody response. *Mol. Cell. Biol.* **26**, 1817-1825.

Clark, K. A., McGrail, M. and Beckerle, M. C. (2003). Analysis of PINCH function in Drosophila demonstrates its requirement in integrin-dependent cellular processes. *Development* **130**, 2611-2621.

Delon, I. and Brown, N. H. (2007). Integrins and the actin cytoskeleton. *Curr. Opin. Cell Biol.* **19**, 43-50.

Devenport, D., Bunch, T. A., Bloor, J. W., Brower, D. L. and Brown, N. H. (2007). Mutations in the Drosophila alphaPS2 integrin subunit uncover new features of adhesion site assembly. *Dev. Biol.* **308**, 294-308.

Dietzl, G., Chen, D., Schnorrer, F., Su, K. C., Barinova, Y., Fellner, M., Gasser, B., Kinsey, K., Oppel, S., Scheiblauer, S. et al. (2007). A genome-wide transgenic RNAi library for conditional gene inactivation in Drosophila. *Nature* **448**, 151-156.

Fukuda, K., Gupta, S., Chen, K., Wu, C. and Qin, J. (2009). The pseudoactive site of ILK is essential for its binding to α-Parvin and localization to focal adhesions. *Mol. Cell* **36**, 819-830.

Geiger, B. and Yamada, K. M. (2011). Molecular architecture and function of matrix adhesions. *Cold Spring Harb. Perspect. Biol.* **3**, a005033.

Gimona, M., Djinovic-Carugo, K., Kranewitter, W. J. and Winder, S. J. (2002). Functional plasticity of CH domains. *FEBS Lett.* **513**, 98-106.

Hannigan, G. E., Leung-Hagesteijn, C., Fitz-Gibbon, L., Coppolino, M. G., Radeva, G., Filmus, J., Bell, J. C. and Dedhar, S. (1996). Regulation of cell adhesion and anchorage-dependent growth by a new β 1-integrin-linked protein kinase. *Nature* **379**, 91-96.

Kadrmas, J. L., Smith, M. A., Clark, K. A., Pronovost, S. M., Muster, N., Yates, J. R., 3rd and Beckerle, M. C. (2004). The integrin effector PINCH regulates JNK activity and epithelial migration in concert with Ras suppressor 1. *J. Cell Biol.* **167**, 1019-1024.

Kiehart, D. P., Ketchum, A., Young, P., Lutz, D., Alfenito, M. R., Chang, X. J., Awobuluyi, M., Pesacreta, T. C., Inoué, S., Stewart, C. T. et al. (1990). Contractile proteins in Drosophila development. *Ann. N. Y. Acad. Sci.* **582**, 233-251.

Kimura, M., Murakami, T., Kizaka-Kondoh, S., Itoh, M., Yamamoto, K., Hojo, Y., Takano, M., Kario, K., Shimada, K. and Kobayashi, E. (2010). Functional molecular imaging of ILK-mediated Akt/PKB signaling cascades and the associated role of beta-parvin. *J. Cell Sci.* **123**, 747-755.

LaLonde, D. P., Brown, M. C., Bouverat, B. P. and Turner, C. E. (2005). Actopaxin interacts with TESK1 to regulate cell spreading on fibronectin. *J. Biol. Chem.* **280**, 21680-21688.

LaLonde, D. P., Grubinger, M., Lamarche-Vane, N. and Turner, C. E. (2006). CdGAP associates with actopaxin to regulate integrin-dependent changes in cell morphology and motility. *Curr. Biol.* **16**, 1375-1385.

Lange, A., Wickström, S. A., Jakobson, M., Zent, R., Sainio, K. and Fässler, R. (2009). Integrin-linked kinase is an adaptor with essential functions during mouse development. *Nature* **461**, 1002-1006.

Langer, C. C., Ejsmont, R. K., Schönbauer, C., Schnorrer, F. and Tomancak, P. (2010). In vivo RNAi rescue in Drosophila melanogaster with genomic transgenes from Drosophila pseudoobscura. *PLoS ONE* **5**, e8928.

Lee, S. and Kolodziej, P. A. (2002). Short Stop provides an essential link between F-actin and microtubules during axon extension. *Development* **129**, 1195-1204.

Legate, K. R., Montañez, E., Kudlacek, O. and Fässler, R. (2006). ILK, PINCH and parvin: the tIPP of integrin signalling. *Nat. Rev. Mol. Cell Biol.* **7**, 20-31.

Li, S., Bordoy, R., Stanchi, F., Moser, M., Braun, A., Kudlacek, O., Wewer, U. M., Yurchenco, P. D. and Fässler, R. (2005). PINCH1 regulates cell-matrix and cell-cell adhesions, cell polarity and cell survival during the peri-implantation stage. *J. Cell Sci.* **118**, 2913-2921.

Lin, X., Qadota, H., Moerman, D. G. and Williams, B. D. (2003). C. elegans PAT-6/actopaxin plays a critical role in the assembly of integrin adhesion complexes in vivo. *Curr. Biol.* **13**, 922-932.

Lorenz, S., Vakonakis, I., Lowe, E. D., Campbell, I. D., Noble, M. E. and Hoellerer, M. K. (2008). Structural analysis of the interactions between paxillin LD motifs and alpha-parvin. *Structure* **16**, 1521-1531.

Mishima, W., Suzuki, A., Yamaji, S., Yoshimi, R., Ueda, A., Kaneko, T., Tanaka, J., Miwa, Y., Ohno, S. and Ishigatsubo, Y. (2004). The first CH domain of affixin activates Cdc42 and Rac1 through alphaPIX, a Cdc42/Rac1-specific guanine nucleotide exchanging factor. *Genes Cells* **9**, 193-204.

Montanez, E., Wickström, S. A., Altstätter, J., Chu, H. and Fässler, R. (2009). Alpha-parvin controls vascular mural cell recruitment to vessel wall by regulating RhoA/ROCK signalling. *EMBO J.* **28**, 3132-3144.

Nakamura, F., Hartwig, J. H., Stossel, T. P. and Szymanski, P. T. (2005). Ca2+ and calmodulin regulate the binding of filamin A to actin filaments. *J. Biol. Chem.* **280**, 32426-32433.

Narasimha, M. and Brown, N. H. (2005). Integrins and associated proteins in Drosophila development. In *Integrins And Development* (ed. E. H. J. Danen). Georgetown, TX, USA: Landes Bioscience.

Nikolopoulos, S. N. and Turner, C. E. (2000). Actopaxin, a new focal adhesion protein that binds paxillin LD motifs and actin and regulates cell adhesion. *J. Cell Biol.* **151**, 1435-1448.

Norman, K. R., Cordes, S., Qadota, H., Rahmani, P. and Moerman, D. G. (2007). UNC-97/PINCH is involved in the assembly of integrin cell adhesion complexes in Caenorhabditis elegans body wall muscle. *Dev. Biol.* **309**, 45-55.

Olski, T. M., Noegel, A. A. and Korenbaum, E. (2001). Parvin, a 42 kDa focal adhesion protein, related to the alpha-actinin superfamily. *J. Cell Sci.* **114**, 525-538.

Parnas, D., Haghighi, A. P., Fetter, R. D., Kim, S. W. and Goodman, C. S. (2001). Regulation of postsynaptic structure and protein localization by the Rho-type guanine nucleotide exchange factor dPix. *Neuron* **32**, 415-424.

Röper, K., Gregory, S. L. and Brown, N. H. (2002). The 'spectraplakins': cytoskeletal giants with characteristics of both spectrin and plakin families. *J. Cell Sci.* **115**, 4215-4225.

Rosenberger, G., Jantke, I., Gal, A. and Kutsche, K. (2003). Interaction of alphaPIX (ARHGEF6) with beta-parvin (PARVB) suggests an involvement of alphaPIX in integrin-mediated signaling. *Hum. Mol. Genet.* **12**, 155-167.

Sakai, T., Li, S., Docheva, D., Grashoff, C., Sakai, K., Kostka, G., Braun, A., Pfeifer, A., Yurchenco, P. D. and Fässler, R. (2003). Integrin-linked kinase (ILK) is required for polarizing the epiblast, cell adhesion, and controlling actin accumulation. *Genes Dev.* **17**, 926-940.

Sebé-Pedrós, A., Roger, A. J., Lang, F. B., King, N. and Ruiz-Trillo, I. (2010). Ancient origin of the integrin-mediated adhesion and signaling machinery. *Proc. Natl. Acad. Sci. USA* **107**, 10142-10147.

Sepulveda, J. L. and Wu, C. (2006). The parvins. *Cell. Mol. Life Sci.* **63**, 25-35.

Torgler, C. N., Narasimha, M., Knox, A. L., Zervas, C. G., Vernon, M. C. and Brown, N. H. (2004). Tensin stabilizes integrin adhesive contacts in Drosophila. *Dev. Cell* **6**, 357-369.

Wang, X., Fukuda, K., Byeon, I. J., Velyvis, A., Wu, C., Gronenborn, A. and Qin, J. (2008). The structure of alpha-parvin CH2-paxillin LD1 complex reveals a novel modular recognition for focal adhesion assembly. *J. Biol. Chem.* **283**, 21113-21119.

Wickström, S. A., Lange, A., Montanez, E. and Fässler, R. (2010). The ILK/PINCH/parvin complex: the kinase is dead, long live the pseudokinase! *EMBO J.* **29**, 281-291.

Wickström, S. A., Radovanac, K. and Fässler, R. (2011). Genetic analyses of integrin signaling. *Cold Spring Harb. Perspect. Biol.* **3**, a005116.

Wolfenson, H., Henis, Y. I., Geiger, B. and Bershadsky, A. D. (2009). The heel and toe of the cell's foot: a multifaceted approach for understanding the structure and dynamics of focal adhesions. *Cell Motil. Cytoskeleton* **66**, 1017-1029.

Wu, C. (2004). The PINCH-ILK-parvin complexes: assembly, functions and regulation. *Biochim. Biophys. Acta* **1692**, 55-62.

Wu, C. and Dedhar, S. (2001). Integrin-linked kinase (ILK) and its interactors: a new paradigm for the coupling of extracellular matrix to actin cytoskeleton and signaling complexes. *J. Cell Biol.* **155**, 505-510.

Yamaji, S., Suzuki, A., Sugiyama, Y., Koide, Y., Yoshida, M., Kanamori, H., Mohri, H., Ohno, S. and Ishigatsubo, Y. (2001). A novel integrin-linked kinase-binding protein, affixin, is involved in the early stage of cell-substrate interaction. *J. Cell Biol.* **153**, 1251-1264.

Yamaji, S., Suzuki, A., Kanamori, H., Mishima, W., Yoshimi, R., Takasaki, H., Takabayashi, M., Fujimaki, K., Fujisawa, S., Ohno, S. et al. (2004). Affixin interacts with α-actinin and mediates integrin signaling for reorganization of F-actin induced by initial cell-substrate interaction. *J. Cell Biol.* **165**, 539-551.

Zaidel-Bar, R., Itzkovitz, S., Ma'ayan, A., Iyengar, R. and Geiger, B. (2007). Functional atlas of the integrin adhesome. *Nat. Cell Biol.* **9**, 858-867.

Zervas, C. G., Gregory, S. L. and Brown, N. H. (2001). Drosophila integrin-linked kinase is required at sites of integrin adhesion to link the cytoskeleton to the plasma membrane. *J. Cell Biol.* **152**, 1007-1018.

Zervas, C. G., Psarra, E., Williams, V., Solomon, E., Vakaloglou, K. M. and Brown, N. H. (2011). A central multifunctional role of integrin-linked kinase at muscle attachment sites. *J. Cell Sci.* **124**, 1316-1327.

Zhang, Y., Chen, K., Tu, Y., Velyvis, A., Yang, Y., Qin, J. and Wu, C. (2002). Assembly of the PINCH-ILK-CH-ILKBP complex precedes and is essential for localization of each component to cell-matrix adhesion sites. *J. Cell Sci.* **115**, 4777-4786.

Zhang, Y., Chen, K., Tu, Y. and Wu, C. (2004). Distinct roles of two structurally closely related focal adhesion proteins, α-parvins and β-parvins, in regulation of cell morphology and survival. *J. Biol. Chem.* **279**, 41695-41705.